JACS
JOURNAL OF THE AMERICAN CHEMICAL SOCIETY
Article
pubs.acs.org/JACS

Modulating Short Wavelength Fluorescence with Long Wavelength Light

Graeme Copley,[†] Jason G. Gillmore,[†,‡] Jeffrey Crisman,[†] Gerdenis Kodis,[†] Christopher L. Gray,[†] Brian R. Cherry,[§] Benjamin D. Sherman,[†] Paul A. Liddell,[†] Michelle M. Paquette,[∥] Laimonas Kelbauskas,[⊥] Natia L. Frank,[∥] Ana L. Moore,*[,†] Thomas A. Moore,*[,†] and Devens Gust*[,†]

[†]Department of Chemistry and Biochemistry, Arizona State University, Tempe, Arizona 85287, United States
[‡]Department of Chemistry, Hope College, Holland, Michigan 49423, United States
[§]Magnetic Resonance Research Center, Arizona State University, Tempe, Arizona 85287, United States
[∥]Department of Chemistry, University of Victoria, Victoria, British Columbia V8W 3 V6, Canada
[⊥]Biodesign Institute, Arizona State University, Tempe, Arizona 85287, United States

Supporting Information

ABSTRACT: Two molecules in which the intensity of shorter-wavelength fluorescence from a strong fluorophore is modulated by longer-wavelength irradiation of an attached merocyanine−spirooxazine reverse photochromic moiety have been synthesized and studied. This unusual fluorescence behavior is the result of quenching of fluorophore fluorescence by the thermally stable, open, zwitterionic form of the spirooxazine, whereas the photogenerated closed, spirocyclic form has no effect on the fluorophore excited state. The population ratio of the closed and open forms of the spirooxazine is controlled by the intensity of the longer-wavelength modulated light. Both square wave and sine wave modulation were investigated. Because the merocyanine−spirooxazine is an unusual reverse photochrome with a thermally stable long-wavelength absorbing form and a short-wavelength absorbing photogenerated isomer with a very short lifetime, this phenomenon does not require irradiation of the molecules with potentially damaging ultraviolet light, and rapid modulation of fluorescence is possible. Molecules demonstrating these properties may be useful in fluorescent probes, as their use can discriminate between probe fluorescence and various types of adventitious "autofluorescence" from other molecules in the system being studied.

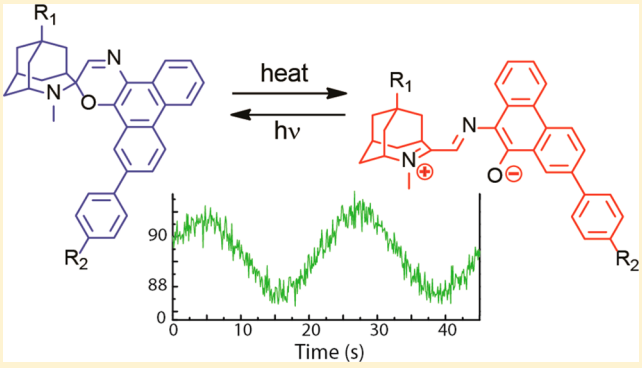

INTRODUCTION

Because fluorescence from probe molecules following excitation with visible or ultraviolet light can be detected with extreme sensitivity and a huge variety of potential fluorophores suitable for different environments exist, fluorescence detection is commonly used in biology, medicine, sensing, tracking, and visualization of many substances, labeling and identification, imaging of many kinds, and so forth. Excitation of a chromophore often leads to fluorescence from the initially excited electronic state, from a lower energy electronic state of the same chromophore into which the first state has relaxed, or from a second chromophore that accepts excitation energy from the first. In all these cases, the emitted light is invariably of the same or longer wavelength than the absorbed light. This fact can cause problems when fluorescence techniques are used for detection or imaging in biomedical or other applications. The light used to excite a fluorescent probe can also excite interfering background fluorescence from other chromophores in the sample that absorb and emit in similar wavelength regimes. Amplitude modulation of the exciting light coupled with phase-sensitive (lock-in) detection of the emission can discriminate against some adventitious light, but not against spurious emission (autofluorescence) resulting from excitation by the modulated beam itself. Luminescence upconversion using some kinds of nanoparticles and related materials can reduce problems with autofluorescence under some conditions,[1] but their applications are limited.

Photochromic molecules exist in two metastable isomeric forms interconvertible by light and often by heat. Several classes of photochromes are known.[2] They all feature one isomeric form with absorption at shorter wavelengths and a second that absorbs at longer wavelengths due to more extended conjugation. Although photochromes have various realized and potential uses on their own,[2] they can also affect the photochemical properties of chemically attached or nearby chromophores through quenching of excited states by energy transfer or photoinduced electron transfer. These interactions

Received: May 15, 2014
Published: July 29, 2014

   dx.doi.org/10.1021/ja504879p | J. Am. Chem. Soc. 2014, 136, 11994−12003

with other chromophores greatly extend the potential applications of photochromes.[3−12]

In the past, we have used photochromes covalently linked to other moieties as the basis for photochemical molecular logic devices (Boolean logic gates, half adders, etc.),[13,14] to control emission from fluorophores,[15,16] and to mimic photoprotective functions in photosynthesis.[17] We recently reported an approach that can in principle eliminate the problems of autofluorescence mentioned above by modulating fluorescence intensity using light of longer wavelength than the emission being observed.[15] This seemingly antithermodynamic result was achieved by controlling fluorescence from five bis-(phenylethynyl)anthracene (BPEA) fluorophores (that emit at ca. 480 nm) with a dithienylethene (DTE) photochromic switch that is isomerized from its closed form to its open form by light at wavelengths > ca. 610 nm. Modulation of the red light modulates the population of the closed DTE, which is in turn able to quench fluorescence from the BPEA (excited at shorter wavelengths) via singlet−singlet energy transfer. The emission from BPEA could be modulated by sine or square wave modulation of the red light, and both frequency modulation and amplitude modulation were observed.

Although this molecule demonstrated the concept of using longer-wavelength light to modulate shorter-wavelength emission, it had several significant drawbacks. First, photoisomerization of the DTE was slow using light of practical intensities, and modulation periods of several hundred seconds were required. This precludes useful phase-sensitive detection. Second, continuous UV light (350 nm) had to be supplied in order to maintain a viable population of the closed (quenching) form of the DTE. This short-wavelength light led to relatively rapid decomposition of the compound, especially in the presence of even small amounts of oxygen. In addition, UV light will not penetrate many types of samples.

These drawbacks are both related to the type of photochrome employed. Most research on photochromes has focused on developing materials that are most thermally stable in their short-wavelength absorbing forms and with slow thermal isomerization rates for the two states. These are the qualities most useful for applications such as self-darkening sunglasses and data storage media. The photochrome used in our previous work was of this type and led to the problems noted.

Herein, we report three new molecular dyads that are designed to address these shortcomings. They make use of unusual reverse photochromes, which are thermally stable in their long-wavelength absorbing forms. In addition, after photochemical conversion to the short-wavelength absorbing forms, they rapidly thermally revert to the long-wavelength state. These properties make them useless for the usual photochromic applications but ideal for our purposes.

One of the new dyads (**1**) consists of a BPEA fluorophore linked to a spiro-[azahomoadamantane-phenanthrolinoxazine] photochrome, and the other two (**2**, **3**) feature a 4,4-difluoro-4-bora-3a,4a-diaza-*s*-indacene (BODIPY) fluorophore linked to a spiro-[azahomoadamantane-phenanthrene] photochrome (Figure 1). The spirooxazines (SO) of **1**, **2**, and **3** exist mainly in the thermally stable open, zwitterionic merocyanine forms ($\mathbf{1}_o$, $\mathbf{2}_o$, $\mathbf{3}_o$) in polar solvents. These forms absorb visible light, and may be photoisomerized to the colorless spirocyclic forms $\mathbf{1}_c$, $\mathbf{2}_c$, and $\mathbf{3}_c$, which rapidly thermally revert to the colored isomers. In all three molecules, the fluorophore component fluoresces strongly when the photochrome is in the closed form. However, this fluorescence is strongly quenched when the spirooxazine component is in the open, merocyanine form, due to rapid singlet−singlet energy transfer to the photochrome.

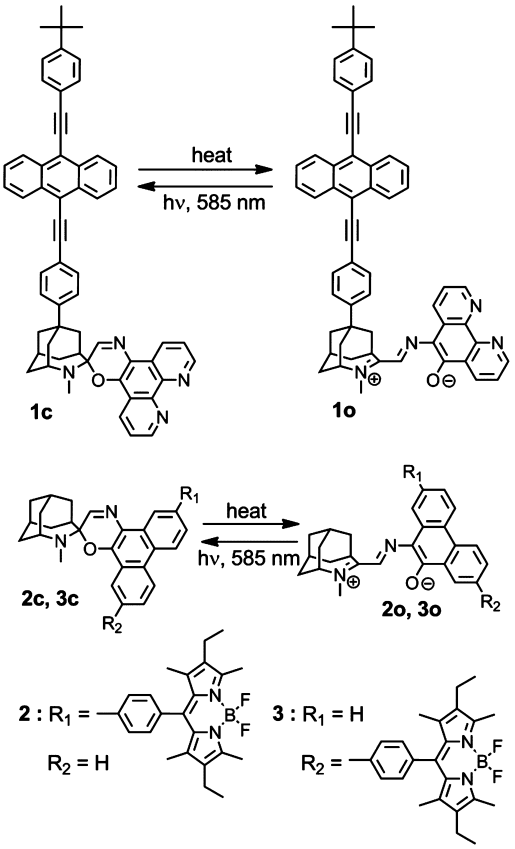

Figure 1. Structures of fluorphore-spirooxazine dyads **1**, **2**, and **3** in the closed, spirocyclic (e.g., $\mathbf{1}_c$) and open, zwitterionic (e.g., $\mathbf{1}_o$) forms.

This photochemistry permits the desired photomodulation effects. As discussed below, fluorescence of the BPEA moiety of **1** is excited by relatively weak steady-state excitation at 440 nm, and emission intensity at 480 nm is modulated by excitation with modulated 585 nm light. In the case of **2** and **3**, fluorescence at 540 nm is excited by steady state irradiation at 500 nm and modulated by excitation at 585 nm. Modulation frequencies are much higher than were obtained with the system reported earlier, and no UV irradiation at all was required, thus eliminating decomposition from this source.

RESULTS AND DISCUSSION

Selection of Chromophores. The BODIPY and BPEA fluorophores were chosen because they have high quantum yields of fluorescence, absorb at shorter wavelengths than the open photochromes, and emit in the region where the open forms of the photochromes absorb, thus meeting the energetic requirements for quenching of the fluorophore excited state by singlet−singlet energy transfer. Identification of a suitable photochrome was more difficult. As mentioned above the majority of known photochromes are thermally stable in their colorless, UV-absorbing forms, and have slow thermal reversion to their most stable forms at ambient temperatures. For the purposes of this study, a reverse photochrome that is most stable in its long-wavelength absorbing form was desired, in order to eliminate the need for potentially destructive UV

dx.doi.org/10.1021/ja504879p | J. Am. Chem. Soc. 2014, 136, 11994−12003

irradiation to maintain a population of the photochrome in the form suitable for quenching the fluorophore. In addition, rapid thermal reversion of the short wavelength absorbing form to the longer-wavelength form was necessary so that relatively rapid modulation of the population was possible. The spiro[azahomoadamantane] spirooxazine photochromes have been found to feature both of these desirable properties.[18]

Synthesis of the Dyads. Rapid singlet−singlet energy transfer from fluorophore to photochrome by the Förster mechanism[19,20] requires reasonably close spatial approach of the two chromophores. This can be achieved by covalently joining the moieties with short linkers. However, adding substituents to photochromes can significantly alter isomer equilibria, isomerization rates, and quantum yields due to electronic perturbations. We initially sought to minimize such effects by linking fluorophores to the spirooxazine via the alkyl substituent on the amine nitrogen (methyl in **1**−**3**). However, the methods we attempted were synthetically incompatible with either the fluorophore or the spirooxazine moiety. Thus, we designed **1**, in which linkage is via the azahomoadamantane, and **2** and **3**, in which the phenanthrene moiety bears the fluorophore. As discussed below, the synthesis of all of these compounds required the use of Pd-catalyzed couplings. It was discovered that these couplings must be executed prior to forming the zwitterionic merocyanines. Carrying out such couplings in the presence of the preformed photochrome failed.

Dyad **1** was synthesized according to the route diagrammed in Figure 2. Bromobenzene was alkylated using commercially available 5-hydroxyadamantan-2-one **4** and trifluoromethanesulfonic acid. The resulting ketone **5** was treated with methylmagnesium iodide to obtain the mixture of alcohols **6**. Ring expansion of the alcohols with sodium azide gave **7**.

For preparation of the BPEA fluorophore, 9-bromoanthraldehyde **8** was coupled to 1-ethynyl-4-*t*-butylbenzene using palladium coupling agents to give aldehyde **9**. Compound **9** was converted to **10** using dimethyl (1-diazo-2-oxopropyl)-phosphonate, and **10** was coupled to **7** using palladium coupling agents to yield **11**.

Methylation of **11** with methyl iodide gave **12**, which was converted to the enamine with triethylamine. Coupling of the enamine with 5-hydroxy-6-nitroso-1,10-phenanthroline as previously described for a related compound gave the desired dyad $\mathbf{1}_o$.[18]

The route for preparation of **2** and **3** is shown in Figure 3. Iodination of 9,10-phenanthrenequinone gave **13**, which was coupled to BODIPY boronic acid pinacol ester[21] **14** using tetrakis(triphenylphosphine)palladium(0) to yield **15**. Diketone **15** was converted to the mixture of nitroso compounds **16** and **17** by treatment with hydroxylamine hydrochloride. The final reaction involved treating 4,5-dimethyl-4-azahomoadamant-4-enium iodide with triethylamine at low temperature to generate 4-methyl-5-methylene-4-azahomoadamantane in situ,[18] followed by addition of 4 Å molecular sieves and the mixture of **16** and **17**. Heating yielded a mixture of **2** and **3**, which were separated by chromatography. Synthetic details for the preparation of all compounds are given in the Supporting Information.

Structure Identification. Dyads **2** and **3** have similar properties and identification required extensive NMR investigation. The dyad later identified as **3** was chosen for study. A combination of ^{1}H−^{1}H COSY and ^{1}H−^{13}C HSQC and HMBC measurements were employed with the molecule dissolved in acetone-d_6, where **3** exists as an equilibrium mixture of the open and closed forms. Figure 4 shows correlations from the COSY and HMBC experiments that allowed identification of $\mathbf{3}_o$ and $\mathbf{3}_c$. Key correlations are those that prove that the BODIPY moiety is linked to the 6-membered ring of phenanthrene that is closest to the oxygen atom. Both ^{1}H and ^{13}C NMR assignments for **3** and representative 2D spectra are given in the Supporting Information.

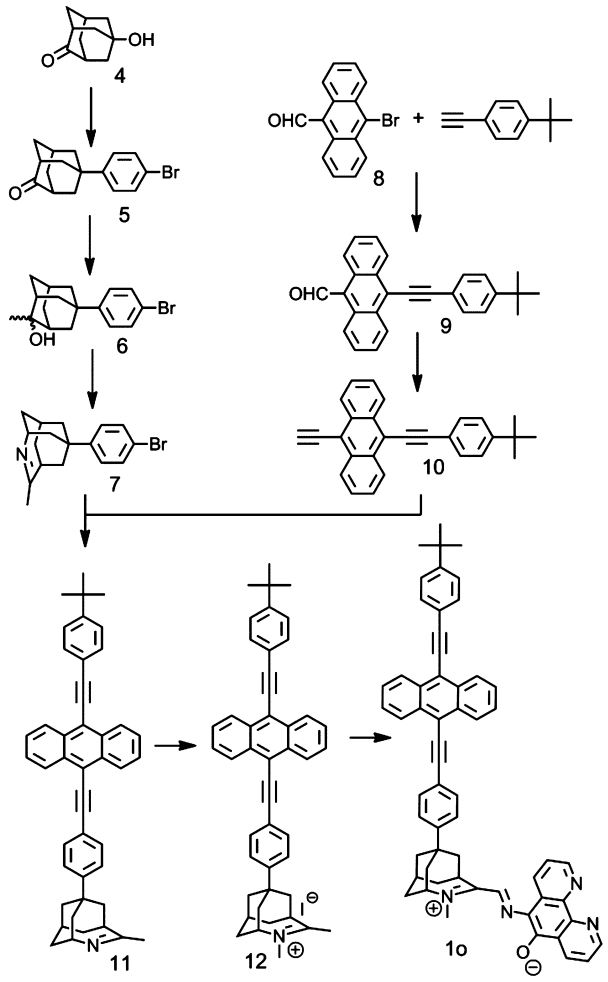

Figure 2. Synthetic route to dyad **1**. Reagents and conditions are given in the Supporting Information.

Electrochemical Data. Cyclic voltammetric investigations were carried out in order to determine whether or not photoinduced electron transfer could play a role in the quenching of the fluorophores. Studies were carried out in distilled acetonitrile containing 0.10 M tetra-*n*-butylammonium hexafluorophosphate as supporting electrolyte. The experiments were performed in a one-compartment cell with a three-electrode configuration consisting of a glassy carbon working electrode, a Pt counter electrode, and an Ag^+/Ag quasireference electrode. Potentials were converted to SCE by using ferrocenium/ferrocene (0.45 V vs SCE). In this solvent, the photochromes are present mainly in the open, zwitterionic forms. Results for **1**, **3**, model BPEA **18**, and model BODIPY **19** (Figure 5) are shown in Table 1. As noted, some of the redox waves were irreversible, and so those values in the table are shown as peak potentials.

The results for model **18** allow assignment of the potentials at 1.20 and −1.36 V observed in **1** to the first oxidation and first reduction of the BPEA moiety, respectively. Thus, the oxidation

dx.doi.org/10.1021/ja504879p | J. Am. Chem. Soc. 2014, 136, 11994−12003

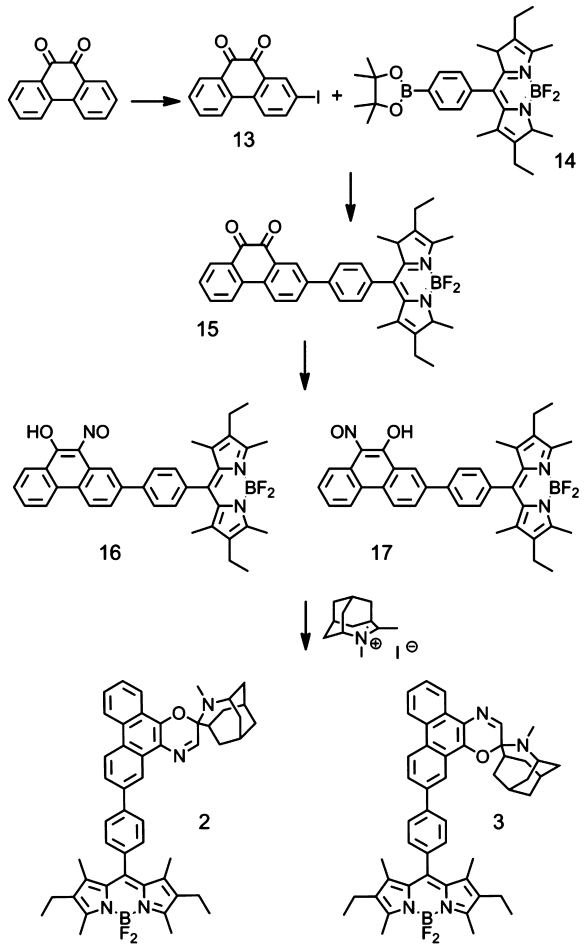

Figure 3. Synthetic route to dyads **2** and **3**. Reagents and conditions are given in the Supporting Information.

of **1** at 0.69 V and the reduction at −0.97 are assigned to the first oxidation and first reduction of the spirooxazine (SO), respectively. On the basis of these results, a potential $BPEA^{\bullet+}$–$SO^{\bullet-}$ state would lie 2.17 eV above the neutral state, and a potential $BPEA^{\bullet-}$–$SO^{\bullet+}$ would reside at 2.05 eV.

Turning now to the BODIPY series of dyads, by referring to model **19**, we assign the oxidation of dyad **3** at 1.07 V and the reduction at −1.18 V to the BODIPY moiety. Thus, the potentials at 0.53 and −1.26 V observed for **3** are assigned to the oxidation and reduction of the SO moiety, respectively. These differ somewhat from those of model compound **20** due to the substitution on the phenanthrene ring.[22] On the basis of these assignments, a potential $BODIPY^{\bullet+}$–$SO^{\bullet-}$ state would be 2.33 eV above the neutral state, and a $BODIPY^{\bullet-}$–$SO^{\bullet+}$ would lie at 1.71 eV.

Photochemistry of Model SO 21. The absorbance spectrum of **21** is strongly solvent dependent, as solvent polarity affects the equilibrium between the open and closed forms. Figure 6a shows the absorption spectrum of **21** in acetonitrile and at the same concentration in cyclohexane. In acetonitrile, the spectrum is dominated by the strong absorbance at 547 nm of the zwitterionic $\mathbf{21}_o$ form. Peaks are also observed at 334, 360 (sh), 465 (sh), and 515 (sh) nm. In cyclohexane, the peak at 547 nm is greatly reduced, as most of the material has converted to the spirocyclic form $\mathbf{21}_c$. This closed form has absorbance at 270 and ca. 350 nm (broad band); there is no absorption at longer wavelengths.

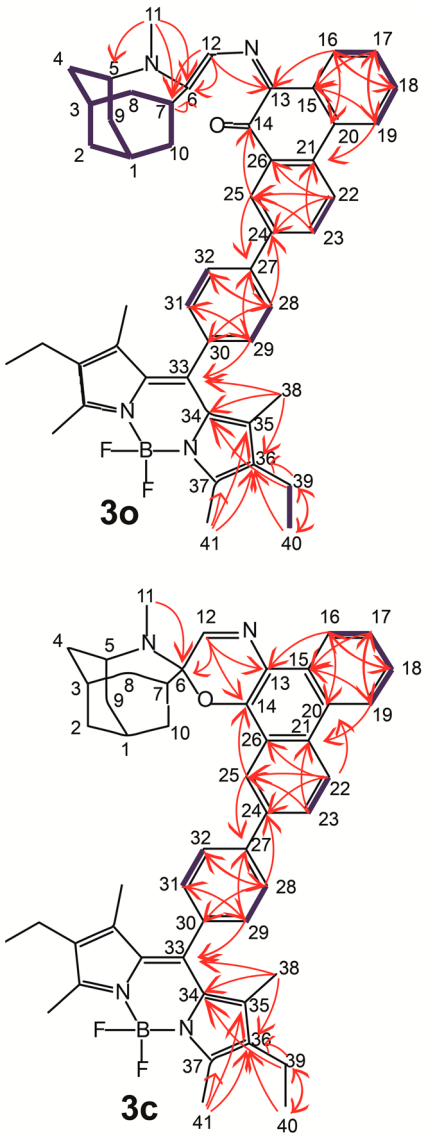

Figure 4. Atomic connectivities for dyad **3** as determined from NMR investigations. The thick lines represent ^1H–^1H COSY correlations and the red arrows show ^1H–^{13}C HMBC connectivities. (a) Correlations for open form $\mathbf{3}_o$. (b) Correlations for closed form $\mathbf{3}_c$.

The model SO **21** in acetonitrile exhibits fluorescence with a maximum at ca. 425 nm arising from the small amount of spirocyclic $\mathbf{21}_c$ that is present. The excited state lifetime of $\mathbf{21}_c$ was determined using the single photon timing technique. The solution was excited at 370 nm, and emission was monitored at 460 nm. The decay was fitted (χ^2 = 1.17) with two exponential components having lifetimes of 17 ps (99% of the decay) and 3.04 ns (1% of the decay that is ascribed to a minor impurity). The open form, 21_o, showed only extremely weak fluorescence at wavelengths longer than 600 nm.

As reported earlier,[18] excitation of $\mathbf{21}_o$ leads to photoisomerization to $\mathbf{21}_c$, which thermally isomerizes back to $\mathbf{21}_o$ on a time scale of seconds. Thus, irradiation of a solution of **21** leads to a photostationary distribution of isomers that depends on the intensity and wavelength of the exciting light and the temperature. The rate constant for thermal isomerization of $\mathbf{21}_c$ to $\mathbf{21}_o$ in acetonitrile at 300 K is reported as[18] 0.023 s^{-1}, which corresponds to a time constant of 43 s.

dx.doi.org/10.1021/ja504879p | J. Am. Chem. Soc. 2014, 136, 11994−12003

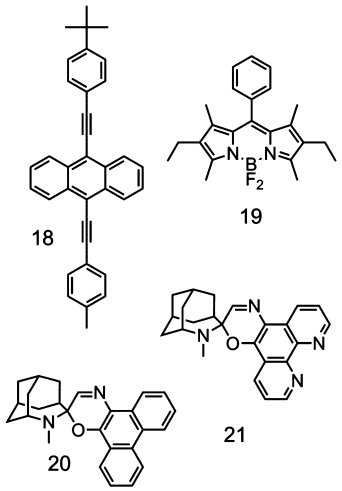

Figure 5. Structures of model fluorophores BPEA (**18**) and BODIPY (**19**) and model spirooxazines **20** and **21**.

Table 1. Redox Potentials for Selected Compounds (V vs SCE)

cmpd	ox_1	ox_2	ox_3	red_1	red_2	red_3
1	0.69 (irr)	0.86 (irr)	1.20 (irr)	−0.97 (irr)	−1.16 (irr)	−1.36
18	1.17 (irr)			−1.33		
3	0.53 (irr)	1.07		−1.18	−1.26	
19	1.07			−1.18		

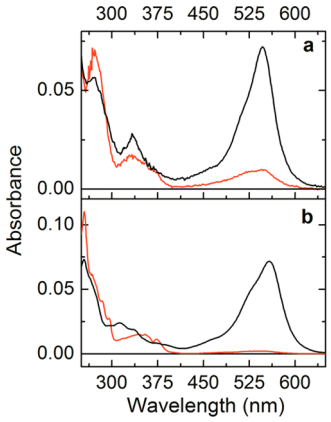

Figure 6. Absorption spectra in acetonitrile (black) and cyclohexane (red) of (a) model SO 21 and (b) model SO **20**.

Photochemistry of 1. In polar solvents such as acetonitrile, BPEA-SO **1** exists mainly in the open, zwitterionic form $\mathbf{1_o}$. Figure 7a shows the absorption spectrum of **1** in that solvent, along with those of **18** and model SO **21**.[18] The BEPA model **18** has absorption maxima at 312, 439, and 464 nm, whereas **21** has maxima at 334, 360 (sh), 465 (sh), 515 (sh) and a strong absorbance at 547 nm. The dyad $\mathbf{1_o}$ has maxima at 313, 333, 441, 465, 515 (sh), and 549 nm. Thus, the spectrum of the dyad is essentially the sum of the spectra of the two component chromophores. The chromophores interact only weakly in absorption. The fluorescence spectrum of the dyad with excitation of (mainly) the BPEA at 400 nm is also shown in Figure 7a. It features maxima at 478, 508, and 545 (sh) nm, and arises from the BPEA chromophore. The BPEA fluorescence has good overlap with the absorption of the SO in the open

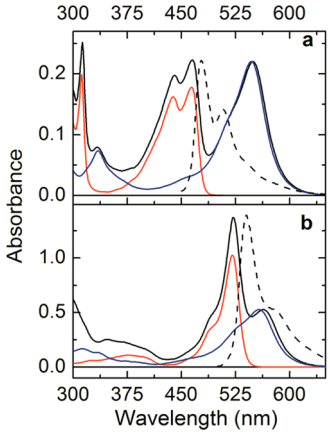

Figure 7. (a) Absorption spectra in acetonitrile of dyad **1** (black), model BPEA **18** (red), and model SO **21** (blue), and fluorescence emission spectrum of dyad **1** with excitation at 400 nm (dashed). (b) Absorption spectra in acetonitrile of dyad **3** (black), model BODIPY **19** (red), and model SO **20** (blue), and fluorescence emission spectrum of dyad **3** with excitation at 400 nm (dashed).

form, and this is an ideal situation for singlet−singlet energy transfer from BPEA to SO.

As was the case with dyad **21**, thermal isomerization of $\mathbf{1_c}$ to $\mathbf{1_o}$ was observed. At 300 K in acetonitrile, the time constant for isomerization, measured by decay of the absorbance at 540 nm when the exciting light was turned off, was 34 s. A minor component ascribed to insufficient sample mixing was also observed. The 34 s time constant is little changed from that for model **21**.

Quenching of BPEA emission by SO in the open form in $\mathbf{1_o}$ was investigated by time-resolved methods in acetonitrile using the single-photon timing method. When BPEA model **18** was excited at 475 nm and its emission was monitored at 560 nm, a single exponential decay was observed with a time constant of 3.68 ns (χ^2 = 1.10). When fluorescence from the BPEA moiety of $\mathbf{1_o}$ was investigated under the same conditions, two time constants were observed: 85 ps (11% of the decay) and 2.80 ns (89%, χ^2 = 1.16). Because **1** exists almost entirely in the $\mathbf{1_o}$ form in this solvent, both decays must be attributed to the open form of the dyad. Both of these time constants are smaller than that of the model BPEA, so that quenching of the BPEA excited singlet state by the open form of SO is confirmed. The observation of two time constants is reasonable because there is considerable rotational freedom about single bonds in the linkages joining the chromophores and within the chromophores themselves. Some of the possible conformations have the transition dipoles nearly perpendicular, which is unfavorable for Förster-type singlet energy transfer. Aggregates may also be present, as the molecules tend to associate due to their high dipole moments. We calculate an amplitude-weighted excited singlet state lifetime of 2.50 ns for the BPEA moieties. The average rate constant for quenching of the BPEA excited singlet state, k_q, is given by eq 1, where τ_{obs} is the lifetime of the BPEA excited state in dyad $\mathbf{1_o}$ and τ_m is the fluorescence lifetime of the BPEA model **18**. From the data above, $k_q = 1.28 \times 10^8\ s^{-1}$. The quantum yield of the quenching process, Φ_q is given by eq 2, and equals 0.32

$$k_q = \frac{1}{\tau_{obs}} - \frac{1}{\tau_m} \quad (1)$$

dx.doi.org/10.1021/ja504879p | J. Am. Chem. Soc. 2014, 136, 11994−12003

$$\Phi_q = k_q \tau_{obs} \quad (2)$$

Modulation Experiments with 1. The experiments above show that the open form of the spirooxazine quenches the excited state of the attached BPEA fluorophore and, thus, reduces the fluorescence quantum yield by 32%. Because irradiation of the open SO isomerizes some of the material to the spirocyclic form, irradiation of the open SO of dyad **1** is expected to increase the quantum yield of fluorescence from the attached BPEA. In order to examine this possibility, we carried out experiments in which we irradiated a sample of $\mathbf{1}_o$ in deaerated acetonitrile solution at 300 K with constant, low intensity blue light at 440 nm in order to elicit BPEA fluorescence, which was monitored at 480 nm. We then also irradiated with light of modulated intensity from a laser providing light in a band of yellow light from 550 to 610 nm in order to modulate the population of $\mathbf{1}_o$ in the sample (see Supporting Information for intensity profile).

Modulation was achieved in two ways. One was via generation of a square wave by a mechanical chopper, giving light of 0 or 10 mW/cm^2 at the sample. Alternatively, the light was modulated as a sine wave by passing linearly polarized laser light through a Glan-type prism polarizer mounted on the hollow axis of a mechanical rotor. Rotation of the prism generated sine wave modulated light of 0−3 mW/cm^2. In each case, the modulated light was brought to the sample in the fluorimeter via an optical fiber to give a 1 cm diameter spot at the sample.

The results of square-wave modulation are shown in Figure 8. Figure 8a shows a portion of one cycle of modulation with a period of 200 s. The BPEA fluorescence excited by the constant intensity 440 nm light is always present, but it is weaker when the yellow light is turned off, because more of $\mathbf{1}_o$, where the SO is in the quenching form, is present. Under the conditions of the experiment, both photoisomerization of $\mathbf{1}_o$ and thermal relaxation of $\mathbf{1}_c$ are rapid enough that the BPEA fluorescence can nearly follow the form of the square wave, although there is still some slow rise when the yellow light is turned on and slow decay when it is turned off. When the period of the square wave is reduced to 16 s (Figure 8b), the isomerizations are no longer able to track the square wave, and so a sawtooth waveform is observed in fluorescence. The modulation depth is reduced relative to Figure 8a because the sample does not have time to reach a steady state value when the light is turned on, or shut off, before the next cycle begins. In Figure 8c, the square wave period is reduced to 9.4 s. When the modulating light cycle is begun, the sawtooth waveform for the fluorescence appears, but the average amplitude of the fluorescence increases until a photostationary distribution of the average populations of the open and closed forms is achieved. Figure 8d shows that when the modulated yellow light is turned off, the BPEA fluorescence decays to its initial value as thermal equilibrium of the open and closed forms is attained.

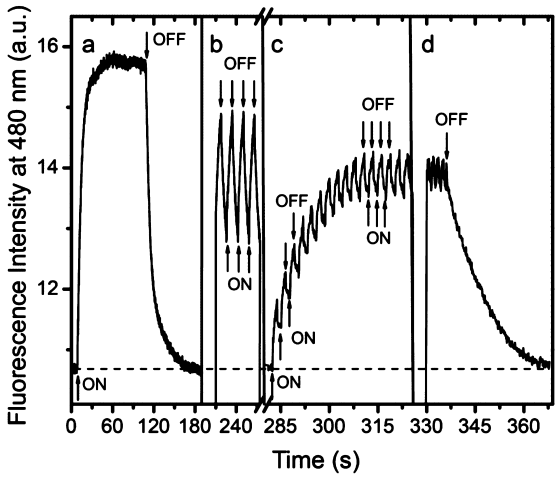

Figure 8. Results of square wave modulation experiments with **1** in acetonitrile at 300 K. Fluorescence of the BPEA moiety at 480 nm (shown here) was elicited by excitation with steady intensity light at 440 nm, and the sample was also excited with square-wave modulated light (550−610 nm) with periods of (a) 200 s, (b) 16 s, (c) 9.4 s. (d) Decay of fluorescence when modulating light is turned off.

The effect of sine wave modulation of the yellow light on blue light fluorescence is shown in Figure 9. The yellow light was modulated with a period of 50 s. The BPEA fluorescence is modulated at the same frequency, but there is a small phase shift, as indicated by the two vertical bars. The phase shift arises because at this frequency, the isomerizations do not quite keep up with the modulation. If the frequency of the modulating yellow light is increased, a sine wave is still observed, although the average amplitude and modulation depth are decreased, and the phase shift becomes larger (results not shown).

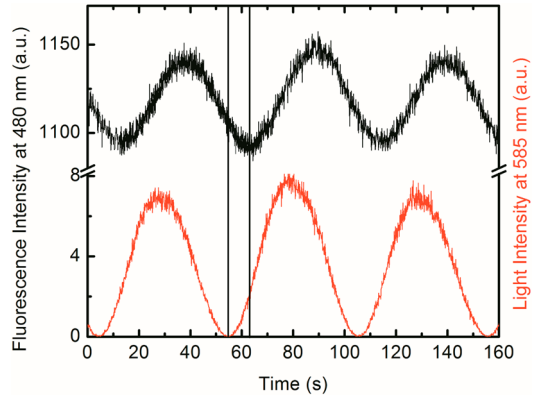

Figure 9. Results of sine wave modulation experiments with **1** in acetonitrile at 300 K. Fluorescence of the BPEA moiety at 480 nm (black) was elicited by excitation with steady intensity light at 440 nm, and the sample was also excited with sine wave modulated light (550−610 nm) with a period of 50 s (red). The vertical lines show the phase shift in the two signals.

The two types of modulation illustrate different facets of dyad behavior and are potentially useful for different applications. Square wave modulation produces a sawtooth type waveform when modulation is much too fast for the photochrome photostationary distribution to track the change in light intensity. Modulation can be observed at much higher frequencies than the actual rates of photo- and thermal isomerizations under a given set of conditions. For example, Figure 8c and d illustrate that modulation with a good signal-to-noise ratio may be obtained with on−off periods of less than 10 s, even though the time constant for thermal isomerization of the photochrome is 43 s. On the other hand, sine wave modulation with frequencies in the vicinity of and lower than the rate constants for thermal and photoisomerization gives an output that reproduces the actual waveform of the modulation light and also allows phase shifting of the signal by specified amounts. These attributes are ideal for the commonly used

dx.doi.org/10.1021/ja504879p | J. Am. Chem. Soc. 2014, 136, 11994−12003

phase-sensitive detectors (lock-in amplifiers), which can achieve signal discrimination even when noise levels are thousands of times higher.

Photochemistry of Model SO 20. The absorbance spectrum of **20** is strongly solvent dependent, as was that of analog **21**. Figure 6b shows the absorption spectrum of **20** in acetonitrile and at the same concentration in cyclohexane. In acetonitrile, the spectrum is somewhat similar to that of **21**, with strong absorbance at 557 nm of the zwitterionic $\mathbf{20}_o$ form. Peaks are also observed at ~320, ~530 (sh), and ~480 (sh) nm. In cyclohexane, the peak at 557 nm is almost absent, as essentially all of the material has converted to the spirocyclic form $\mathbf{20}_c$, which has absorbance at 255 and ca. 350 nm (broad band).

In acetonitrile, SO **20** exhibits fluorescence with a maximum at ~410 nm arising from the small amount of spirocyclic $\mathbf{20}_c$ that is present. The excited state lifetime of $\mathbf{20}_c$ was determined using the single photon timing technique. The solution was excited at 370 nm, and emission was monitored at 460 nm. The decay was fitted ($\chi^2 = 1.16$) with three exponential components having lifetimes of 50 ps (80% of the decay), 470 ps (17%), and 6.60 ns (3% of the decay that is ascribed to a minor impurity). As was the case with **21**, the open form, $\mathbf{20}_o$, showed only very weak fluorescence at wavelengths longer than 600 nm.

As with **21**, SO $\mathbf{20}_o$ undergoes photoisomerization to $\mathbf{20}_c$, which then rapidly thermally isomerizes back to the open form. In order to measure the thermal isomerization time constant, a solution of **20** in acetonitrile at 300 K was illuminated for 60 s with 10 mW of 550−610 nm light, and isomerization to the open form was monitored spectroscopically at 540 nm. The time constant for thermal opening was 3.5 s, which is more than 10 times smaller than that for **21**.

Photochemistry of 3. For the second series of dyads, only the photochemistry of **3** will be discussed. Dyad **2** behaves very similarly, and it was not studied in detail. The absorption spectrum of BODIPY-SO dyad **3** in acetonitrile, where it is present mainly in the open form $\mathbf{3}_o$, is shown in Figure 7b. This figure also gives the spectra of model BODIPY **19** and model spirooxazine **20**. BODIPY **19** has absorption maxima at ~380 (broad), ~495 (sh), and 521 nm. The SO in the open form has absorption at ~320 (broad), ~530 (sh), and 557 nm. The spectrum of the dyad $\mathbf{3}_o$ has maxima at ~370 (broad), ~495 (sh), 522, and 564 nm. Thus, the long wavelength SO band in the dyad is shifted to longer wavelengths by about 7 nm due to interaction with the attached BODIPY chromophore. However, the spectral perturbations due to linking the chromophores are generally small. Excitation of the solution at 400 nm gave rise to fluorescence from the BODIPY at 540 and 577 (sh) nm. As was the case with $\mathbf{1}_o$ the BODIPY emission overlaps well with the absorption of the SO, and the molecule is energetically well poised for singlet−singlet energy transfer from BODIPY to the open SO.

Thermal isomerization of $\mathbf{3}_c$ to $\mathbf{3}_o$ was observed. At 300 K in acetonitrile, the time constant for isomerization was 4.4 s, which is similar to the value of 3.5 s found for **20.**

Time resolved fluorescence studies of $\mathbf{3}_o$ and model **19** were carried out in order to quantify any quenching of the BODIPY excited singlet state by the open SO. Compound **19** in acetonitrile was excited at 475 nm, and emission was monitored at 560 nm. The fluorescence decayed as a single exponential ($\chi^2 = 1.19$) with a time constant of 6.33 ns. When dyad **3** was excited and emission monitored at the same wavelengths, three exponentials were necessary to satisfactorily ($\chi^2 = 1.18$) fit the data: 57 ps (29%), 660 ps (7%), and 4.35 ns (64%). As with dyad **1**, the multiple exponentials are postulated to arise from different conformations of the molecule arising from rotations about single bonds. The amplitude average lifetime is 2.85 ns. Using this number, eq 1 and 2 were employed to calculate an average rate constant for quenching k_q of 1.93×10^8 s^{-1} and a quenching quantum yield Φ_q of 0.55.

Modulation Experiments with 3. Using the apparatus described above, a sample of **3** in deaerated acetonitrile at 300 K was irradiated with constant light at 500 nm to elicit fluorescence from BODIPY (monitored at 540 nm) and also irradiated with yellow light (550−610 nm, 10 mW maximum) that was modulated with a square wave. As can be seen in Figure 10a, when the period of the modulation was 80 s, the fluorescence described a near square wave of the same period. When the period was reduced to 1.0 s (Figure 10b), the fluorescence was modulated as a distorted square wave of the same period and reduced modulation depth. Also, there was an induction period after the modulation was turned on, during which time the sample reached an average photostationary distribution. When the modulating light was turned off, the BPEA fluorescence decays, ultimately to the initial level, as the SO thermally isomerizes back to the open form.

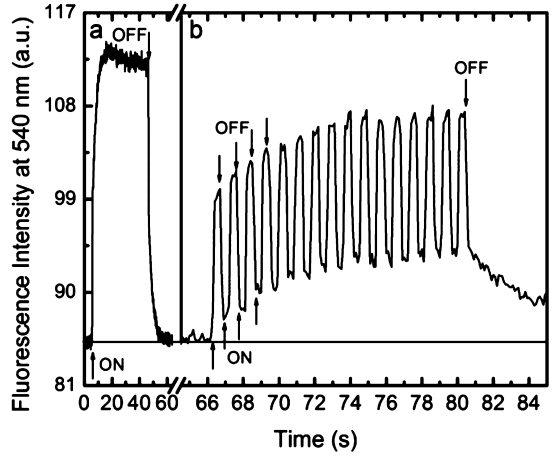

Figure 10. Results of square wave modulation experiments with **3** in acetonitrile at 300 K. Fluorescence of the BODIPY moiety at 540 nm (shown here) was elicited by excitation with steady intensity light at 500 nm, and the sample was also excited with square-wave modulated light (550−610 nm) with periods of (a) 80 s and (b) 1 s.

Figure 11a shows the results of modulation of the same solution with a sine wave of yellow light (550−610 nm, 0−3 mW) with a period of 23 s. The BODIPY fluorescence is modulated in a sine wave of the same frequency. Modulation of the yellow light at a frequency of 3.6 s results in BODIPY fluorescence with a sine wave of the same period, but lower amplitude and smaller modulation depth (Figure 11b).

Quenching Mechanism. Both $\mathbf{1}_o$ and $\mathbf{3}_o$ demonstrate significant quenching of the fluorophore excited state by the open form of the spirooxazine, but not by the closed form, which allows for the observed modulation effects. In principle, this quenching could be due either to singlet−singlet energy transfer from the first excited singlet state of the fluorophore to the open form of the SO or to photoinduced electron transfer involving the two chromophores.

For **1**, the BPEA first excited singlet state lies 2.63 eV above the ground state based on the wavenumber-average of the

dx.doi.org/10.1021/ja504879p | J. Am. Chem. Soc. 2014, 136, 11994−12003

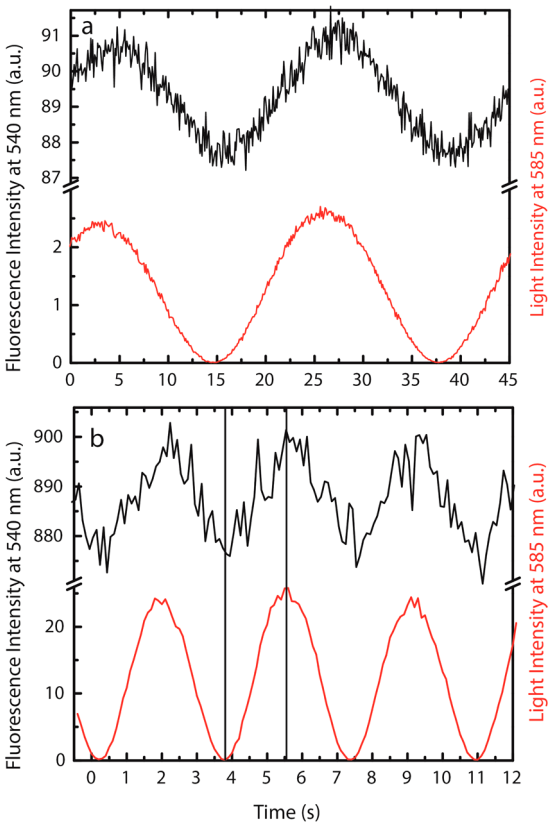

Figure 11. Results of sine wave modulation experiments with **3** in acetonitrile at 300 K. Fluorescence of the BODIPY moiety at 540 nm (black) was elicited by excitation with steady intensity light at 500 nm, and the sample was also excited with sine wave modulated light (550–610 nm, red). (a) Modulation period of 23 s. (b) Modulation period of 3.6 s. The vertical lines in (b) are an aid in observing the lack of significant phase shift in these experiments.

longest-wavelength absorption band maximum (465 nm) and the shortest-wavelength fluorescence band (478 nm). As mentioned above, a $BPEA^{\bullet+}$–$SO^{\bullet-}$ state would lie at 2.17 eV above the neutral state, and a potential $BPEA^{\bullet-}$–$SO^{\bullet+}$ would reside at 2.05 eV. Thus, excited state quenching by photoinduced electron transfer to yield one of these states is thermodynamically possible. On the other hand, as shown in Figure 7a, there is excellent overlap between the BPEA emission and the SO absorption in the open form, and so singlet–singlet energy transfer quenching is also thermodynamically favorable. Photoinduced electron transfer requires orbital overlap of the donor and acceptor. In **1**, there are four single bonds in the linkage between the two chromophores, which would be expected to make photoinduced electron transfer by a superexchange mechanism slow. Thus, although we cannot definitively identify the quenching mechanism, singlet energy transfer by the Förster dipole–dipole mechanism appears to be more likely. The fact that the decay of BPEA fluorescence in $\mathbf{1}_o$ features several lifetimes is consistent with Förster transfer in a molecule with several conformations.

Turning now to $\mathbf{3}_o$, the energy of the first excited singlet state of the BODIPY fluorophore is 2.02 eV above the ground state. A $BODIPY^{\bullet+}$–$SO^{\bullet-}$ state would be 2.33 eV above the ground state, and a $BODIPY^{\bullet-}$–$SO^{\bullet+}$ would lie at 1.71 eV. Thus, quenching by photoinduced electron transfer to yield $BODIPY^{\bullet-}$–$SO^{\bullet+}$ is thermodynamically possible. The excellent overlap of BODIPY emission and open spirooxazine absorption shown in Figure 7b coupled with the close approach of the two π-electron systems suggests that energy transfer should also be favorable. Thus, for $\mathbf{3}_o$, either a quenching mechanism or a combination of the two processes may be responsible for the quenching. The multiexponential nature of the BODIPY decay is more consistent with energy transfer in a molecule with multiple conformations than with electron transfer through the bonds. Although obtaining the fluorescence excitation spectrum for open SO emission in the dyad would in principle allow detection of energy transfer, the fluorescence quantum yield is too low to permit reliable measurements.

The quantum yield of the quenching process is lower for $\mathbf{1}_o$ (0.32) than for $\mathbf{3}_o$ (0.55). Assuming that the quenching in both cases is energy transfer, as discussed above, it is clear from Figure 7 that although the spectral overlap of donor emission and acceptor absorption is good for Förster-type singlet–singlet energy transfer in both compounds, it is better for $\mathbf{3}_o$ than for $\mathbf{1}_o$. In addition, the center-to-center separation of the chromophores is smaller for $\mathbf{3}_o$ and this will contribute to a faster rate. On the other hand, the orientation of the transition moments for both molecules is close to perpendicular, which likely contributes to the relatively low quantum yields for both molecules, given the distances and spectral overlaps involved.

Both dyads may be cycled many times between the open and closed forms in the absence of oxygen. Thus, whatever the quenching mechanism, the resulting species must rapidly return to a ground state rather than lead to decomposition of the material.

■ CONCLUSIONS

Both BPEA-spiro-[azahomoadamantane-phenanthrolinoxazine] dyad **1** and BODIPY-spiro-[azahomoadamantane-phenanthrene] dyad **3** exhibit the properties they were designed to display. Both exist in a thermally stable state in which the spirooxazine moiety is in the open, zwitterionic form, which absorbs yellow-red light. Both rapidly photoisomerize to the spirocyclic form that does not absorb at wavelengths longer than ~400 nm, and both feature rapid thermal isomerization of the spirocyclic form back to the open form. The BPEA and BODIPY moieties are both strongly fluorescent, and the excited states of both are strongly quenched by the spirooxazine in the open, but not in the closed, form. Because of these properties, illumination of either molecule with modulated yellow or red light absorbed by the open SO leads to modulation of the blue fluorescence of the fluorophore. Thus, with either molecule, phase-sensitive detection of fluorophore emission allows detection of fluorescence without interference by extraneous light or by adventitious fluorescence of materials excited by either the steady-state light that elicits fluorescence or the modulation light. Any adventitious fluorescence excited by the shorter-wavelength steady-state light would not be modulated and, therefore, not detected. Any adventitious fluorescence excited by the modulation light would necessarily be at longer wavelengths than the detection wavelength and also would not interfere.

Unlike molecules we have reported earlier,[15] these new systems are based on reverse photochromes and, therefore, do not require illumination with UV light in order to function. This eliminates photodecomposition caused by such UV irradiation. However, the molecules do react with oxygen when illuminated and eventually decompose if oxygen is present during the irradiations. If oxygen is excluded by multiple freeze–thaw cycles under vacuum, both molecules

dx.doi.org/10.1021/ja504879p | J. Am. Chem. Soc. 2014, 136, 11994–12003

may be cycled between the two isomeric states many times using yellow or red light.

In spite of the similarities of the two dyads, there are interesting differences between them. The thermal reversion rate for the spiro-[azahomoadamantane-phenanthrene] found in **3** and model **20** is more than 10 times faster than the corresponding rate for the spiro-[azahomoadamantane-phenanthrolinoxazine] component of **1** and **21**. As described elsewhere,[22] the thermal relaxation rate in photochromes of this type is inversely linearly correlated with the charge-separated character of the open form. Three resonance forms contribute to the structure of the open, merocyanine isomer; a localized neutral form (quinoidal) and two zwitterionic states with different degrees of charge separation. In **20**, the open form has a greater contribution from the neutral resonance structure than it does in **21**. This, in turn, leads to a lower barrier to a cis−trans isomerization step in the reversion process and, thus, to the faster thermal reversion rate.

This allows the modulation of blue fluorescence from the BODIPY of **3** to track the shape and phase of the waveform of the modulating yellow light at much higher frequencies than is possible with **1**. Thus, **3** would be a better candidate for practical application in fluorescence detection than **1**. As shown in Figure 11b, sine waves with a period of only a few seconds or less could be employed. With square wave modulation, sawtooth waveforms of even higher frequency could be detected. Of course, under a given set of irradiation conditions, higher frequency modulation leads to weaker average emission and a smaller modulation depth because the dyad solutions are not able to fully isomerize during one cycle.

The modulation frequencies attainable are strongly dependent upon the light intensity, which affects the rate of photochemical closing of the SO, and the temperature, which controls the thermal reversion to the open form. For the experiments described here, thermal reversion is especially limiting. At higher temperatures, faster modulation would be possible. For both **1** and **3**, modulation frequencies at ambient temperatures are much higher than those that could be obtained with a previously reported system.[15]

As discussed above, the open, photomerocyanine isomers of the photochromes have contributions from three resonance forms. The relative contributions of these forms and the degree of bond localization and charge separation depend on solvent polarity. While the fraction of the open form at equilibrium increases with polarity, photoinduced and thermal isomerization still readily take place in nonpolar media (e.g., toluene).[18] Thus, modulation of fluorescence quenching in the dyads would take place in both hydrophobic and polar environments, although the amount of quenching in a given sample of material would be a function of the fraction of the open form present in the absence of modulating light.

These dyads are not water-soluble. Thus, their use in an aqueous environment would require either structural modification to add solubilizing groups or encapsulation in micelles or similar approaches.

The differences in the absorption spectra also affect the performance. In $\mathbf{1}_o$, the absorption maxima of the BPEA moiety and the longest-wavelength absorption maximum of the open SO are well separated, which makes it relatively simple to irradiate mainly the BPEA with the beam that excites fluorescence and only the SO with the modulation light. This is a a bit more difficult with **3** because the absorption maxima are closer together. The constant intensity shorter-wavelength light that elicits fluorescence will drive a fraction of the open SO into the closed form. However, this effect is not large because the excitation light is weak, and the BODIPY absorbs most of the light.

Also, care must be taken to be certain that the modulating light does not enter the fluorescence detector, or it can be mistaken for fluorescence from the fluorophore. In a fluorimeter, this can be achieved by using a modulating illumination beam at right angles to the fluorescence monochromator and detection. In other contexts, modulation with a narrow-band laser coupled with fluorescence detection at a wavelength different from that of the laser would achieve this end. In the experiments described here, the relatively broad band modulation light that was employed as a suitable narrow-band source was not available.

The dyads described here are optical, molecular analogs of triode vacuum tubes or transistor amplifiers. For example, with **1**, the steady-state 440 nm light corresponds to the input of a transistor, the 480 fluorescence emission to the output, and the 550+ modulated light to the gate voltage.

The ability to modulate short-wavelength fluorescence with longer-wavelength light opens the door to extremely sensitive fluorescence detection without interference from "autofluorescence" or other adventitious light, including fluorescence initiated by both the light beam that excites the fluorophore and the modulating light. Such methods can be useful in biomedical or (nano)technological labeling and detection experiments, fluorescence detection at long distances, and so forth. The results reported here use reverse photochromes bearing fluorescent "beacons" to demonstrate the implementation of this concept.

■ ASSOCIATED CONTENT

Supporting Information

Details of synthesis and characterization, experimental details for spectroscopic and electrochemical studies, and spectroscopic data that was not included in the text. This material is available free of charge via the Internet at http://pubs.acs.org.

■ AUTHOR INFORMATION

Corresponding Authors

gust@asu.edu.
amoore@asu.edu.
tmoore@asu.edu.

Notes

The authors declare no competing financial interest.

■ ACKNOWLEDGMENTS

This work was supported by a grant from the U. S. National Science Foundation (CHE-0846943). J.G.G. was supported by a CAREER grant from the U. S. National Science Foundation (CHE-0952768).

■ REFERENCES

(1) Zhou, J.; Liu, Z.; Li, F. *Chem. Soc. Rev.* **2012**, *41*, 1323−1349.
(2) Crano, J. C.; Guglielmetti, R. J. *Organic Photochromic and Thermochromic Compounds*; Plenum Press: New York, 1999.
(3) Raymo, F. M.; Tomasulo, M. *Chem. Soc. Rev.* **2005**, *34*, 327−336.
(4) Myles, A. J.; Branda, N. R. *J. Am. Chem. Soc.* **2001**, *123*, 177−178.
(5) Haupl, T.; Zimmermann, T.; Hermann, R.; Brede, O. *J. Phys. Chem. A* **1999**, *103*, 6904−6910.
(6) Myles, A. J.; Gorodetsky, B.; Branda, N. R. *Adv. Mater.* **2004**, *16*, 922−925.

(7) Yildiz, I.; Raymo, F. M. *J. Mater. Chem.* **2006**, *16*, 1118−1120.
(8) Raymo, F. M.; Tomasulo, M. *J. Phys. Chem. A* **2005**, *109*, 7343−7352.
(9) Raymo, F. M.; Tomasulo, M. *Chem. Soc. Rev.* **2005**, *34*, 327−336.
(10) Tomasulo, M.; Deniz, E.; Alvarado, R. J.; Raymo, F. M. *J. Phys. Chem. C* **2008**, *112*, 8038−8045.
(11) Remon, P.; Hammarson, M.; Li, S.; Kahnt, A.; Pischel, U.; Andreasson, J. *Chem.—Eur. J.* **2011**, *17*, 6492−6500.
(12) Metivier, R.; Badre, S.; Meallet-Renault, R.; Yu, P.; Pansu, R. B.; Nakatani, K. *J. Phys. Chem. C* **2009**, *113*, 11916−11926.
(13) Gust, D.; Andreasson, J.; Pischel, U.; Moore, T. A.; Moore, A. L. *Chem. Commun.* **2012**, *48*, 1947−1957.
(14) Gust, D.; Moore, T. A.; Moore, A. L. *Chem. Commun.* **2006**, *2006*, 1169−1178.
(15) Keirstead, A. E.; Bridgewater, J. W.; Terazono, Y.; Kodis, G.; Straight, S.; Liddell, P. A.; Moore, A. L.; Moore, T. A.; Gust, D. *J. Am. Chem. Soc.* **2010**, *132*, 6588−6595.
(16) Frey, J.; Kodis, G.; Straight, S. D.; Moore, T. A.; Moore, A. L.; Gust, D. *J. Phys. Chem. A* **2013**, *117*, 607−615.
(17) Straight, S. D.; Kodis, G.; Terazono, Y.; Hambourger, M.; Moore, T. A.; Moore, A. L.; Gust, D. *Nat. Nanotechnol.* **2008**, *3*, 280−283.
(18) Patel, D. G.; Paquette, M. M.; Kopelman, R. A.; Kaminsky, W.; Ferguson, M. J.; Frank, N. L. *J. Am. Chem. Soc.* **2010**, *132*, 12568−12586.
(19) Förster, T. *Ann. Phys.* **1948**, *2*, 55−75.
(20) Förster, T. *Discuss. Faraday Soc.* **1959**, *27*, 7−17.
(21) Chaudhuri, D.; Wettach, H.; van Schooten, K. J.; Liu, S.; Sigmund, E.; Hoeger, S.; Lupton, J. M. *Angew. Chem., Int. Ed.* **2010**, *49*, 7714−7717.
(22) Kurimoto, A.; Paquette, M. M.; Patrick, B. O.; Patel, D.; Frank, N. L. *J. Phys. Chem. A* **2014**, submitted for publication.